ESD response to referees

A.A. Sipos, G. Domokos, J. Török

January 10, 2021

1 Response to Prof. Furbish

We would like to thank Professor Furbish for a thorough and encouraging review. His comment about riverbed collisions was an eye-opener. Below we address all the issues raised in the report.

1. **APPLICATION OF THE MODEL TO ABRASION IN RIVERS**
   We propose to add a new subsection, after Subsection 2.4, where we discuss how our model can be explored to make predictions about fluvial environments. Here follows the suggested subsection:

   ### Fluvial abrasion

   ### 1.1 Fluvial abrasion

   Here we interpret the intuitive picture of fluvial abrasion in the context of our statistical model. In our model a fluvial environment may be represented by a *fluvial population*, consisting of $N+1$ particles: a very large number (N) of small particles X^i ($i = 1, 2, \dots N$) representing the pebbles carried by the river and one very large particle Y representing the riverbed. Such a scenario can not be explored directly in the context of our continuum model, however, as we will discuss in detail in Subsection 3.3, the discrete model can capture this situation even in the limit as $N \to \infty$.

   To make a meaningful characterization of geologically relevant scenarios, we will regard two extreme cases which represent brackets on geological processes. In both cases we assume that the mass evolution is driven by binary collisions and we regard the limit as $N, Y \to \infty$ (while the masses X^i of the small particles remain finite). Since we are interested in the mass evolution of pebbles (and in the current paper we are not interested in the mass evolution of the riverbed) we will denote the relative variance of the pebble population (i.e. all X^i particles, the riverbed Y not included) by $R(t)$. Our aim is to establish the sign of $R_t(t)$ as the main qualitative feature of collective dynamics.

In the first extreme scenario we assume that particles are chosen uniformly from the full *fluvial population*: i.e., the riverbed has no special role. In this case *almost all* collisions will happen among a pair of small particles (X^i, X^j) thus the presence of the riverbed has no impact on the evolution of $R(t)$. For this extreme case all predictions of our continuum model remain valid: $r = 0.5$ will be a critical parameter value above which we see focusing ($R_t < 0$), below which we see dispersing ($R_t > 0$) behaviour. At the critical value $r = 0.5$ our model predicts neutral behaviour with $R_t = 0$.

In the second extreme scenario we assume that the small particles *exclusively* collide with the riverbed (large particle), i.e., we only have (X^i, Y)-type collisions. This means that the evolution for each of the small particles is an identical, independent two-particle process governed by the model (1)-(2) for binary collisional mass evolution. In this process, in the $Y \to \infty$ limit each individual small particle X^i will thus evolve as

$$X^i(t) = X^i(0)e^{-t} \tag{11}$$

and thus follow Sternberg's Law. It is easy to show that for any initial distribution for the masses $X^i(0)$, in this process we have $R_t = 0$. The large Y-particle (riverbed) will lose some mass as well but in this publication we are not interested in that part of the process.

Intuitively it is clear that any geologically relevant process is in-between the above two extreme cases and, although we do not deliver a rigorous proof, it appears plausible that in a geologically relevant setting R_t will be also bounded by the two evolutions predicted for the two extreme scenarios. As for the second extreme scenario we have $R_t = 0$ we expect that for any intermediate scenario the sign of R_t will agree with the sign of R_t based on the first extreme scenario. This would imply that all our qualitative predictions remain valid in fluvial environments.

2. **ESTIMATE FOR EXTREMAL r VALUE**. We propose to add a new Appendix (Appendix D) where we explain our estimate for the parameter r in case of smooth gradient flows (laminar flows). Here follows the suggested Appendix:

Estimating physically possible values of r

In the paper we assumed that the particle collision probability depends on the volume of the particles as

$$P(X) \propto X^r. \tag{D1}$$

Here we investigate two extreme scenarios, associated with the collision probabilities $P_{\mathrm{smooth}}(X)$ and $P_{\mathrm{turbulent}}(X)$ where we expect r to assume its extreme values.

The first is the smooth gradient flow. In such a case the driving fluid has a strong, but on a particle-size scale constant velocity gradient in one of the spatial directions. Such situations may arise, e.g., in shallow water layers. Here the relative velocity of the particles grows with the distance. If we are at distance u from the center of the particle in the direction of the flow velocity gradient, the collision probability $P_{\text{smooth}}(X)$ can be estimated by the product of the velocity difference and the linear cross-section of the particles. (Note that $R \equiv X^{1/3}$ is the linear size of the particle):

$$P_{\text{smooth}}(X) \sim \frac{1}{R}\int_0^R u\sqrt{R^2 - u^2}du = \frac{1}{3}R^2 = \frac{1}{3}X^{2/3}. \qquad \text{(D2)}$$

Based on (D1), this gives us an estimate for high $r = 2/3$.

The other extreme case is a fully chaotic motion where equipartition takes place [Uberoi, 1957]. Thus the kinetic energy of the particles ($\frac{1}{2}\rho X v^2$) is independent of their volume. Thus the speed of the particles must be proportional to $X^{-1/2}$. If we disregard correlations the particles have a cross-section proportional to their projected area which is proportional to $X^{2/3}$. Combining the two gives us

$$P_{\text{turbulent}}(X) \sim X^{-1/2}X^{2/3} = X^{1/6} \qquad \text{(D3)}$$

and based on (D1) we obtain $r = 1/6$. Thus it is possible to have physical scenarios apparent in nature where the value of r falls to either side of the critical value of $r_c = 0.5$ with large enough margin.

3. **DIFFUSION**

   The referee is right, we have used the term 'diffusion' incorrectly. We modified the text in Subsection 2.2., the new version is below.

   Note that contrary to the majority of Fokker-Planck models, our model contains solely the advection term, which readily follows from the deterministic nature of the kernel. Here we aim to figure out the collective behavior implied by (7). Nonetheless, a stochastic kernel would produce diffusion in the master equation, such a generalization might be essential for testing model predictions against experimental data.

2 Response to Dr. Bertoni

While our paper is admittedly a theoretical model, still, its main goal is to offer a new toolkit to geologists. It is reassuring to know that this approach was vetted by an expert field geologist and we would like to sincerely thank Dr. Bertoni for his comments.

We very much appreciate his positive opinion on the problem statement and result discussion. This gives us hope that field experts may, in the future, engage in exploring this interesting subject.

Our referee raises the question how our theoretical predictions may be tested. While we regard this as a key issue, we did not elaborate on this aspect since no testing has been done so far. Still, some of the potential testing strategies appear to be quite clear as we discuss it below.

Our model can be tested at two levels:

(a) at the *input level*, i.e. by testing the kernel and

(b) at the *output level*, i.e. by testing pebble size distributions.

To perform (a), one would need time evolutions for full mass distributions. We are not aware of any such publicly available dataset. To obtain such data the best options appear to be either laboratory flume or drum experiments or, in the field, radio-tagged pebble experiments.

To perform (b), one would need size dependence of abrasion rates. Such an experiment is reported in Figure 9/a of [Attal and Lavé, 2009] and we fitted our kernel to their data.

We discuss these testing options in Subsection 1.4 of the modified manuscript and we included the (b)-type kernel fit in the new Appendix A. Here we found that the experimental data is in fair agreement with our kernel.

In addition we remark that in all experiments the validity depends on the ability of the experimenter to make measurements on the same particle population. To make the experiments consistent with this study, the most straightforward approach is to track the evolution R(t) of the relative variance.

(1) Tumbler experiments. In this case the validity of the experiment is automatically guaranteed. The energy level of the experiment may be controlled either by adjusting the speed or by adding water. Recording $R(t)$ at a wide range of energy levels may help to confirm some aspects of the presented theory.

(2) Flume experiments. Here again, the validity of the experiment is guaranteed. Circular flumes may be adequate testing platforms for lower energy levels.

(3) Field experiments. In this case both the validity and consistency of the experiment is a hard question. The most plausible option are radio-tagged particles, however, low recovery rates may prohibit a reliable monitoring of $R(t)$.

The referee also raises the question whether and to what extent our theory may help to distinguish between coastal and fluvial environments. The question is justified, yet, in the absence of experimental results, a full answer is lacking. Still, this question may be a main motivation behind the design of targeted experiments. Based alone on the predictions of the paper, focusing and dispersing behavior may be present both in a fluvial and in a coastal setting. Focusing processes operate at lower energy levels: this may characterize the lower reaches of rivers as well as wave-current-driven frictional abrasion in coastal environments.

These are the scenarios where our theory predicts that abrasion and transport act in a similar manner on mass distributions. On the other hand, high energy levels indicate dispersing processes where abrasion and transport are counteracting. Such scenarios may be observed in the upper reaches of rivers as well on high-energy beaches often visited by storms. As we can see, at higher energies both transport and abrasion operate much faster and it is a truly challenging question to find out which of these natural processes dominates. Our study offers a tool to make a meaningful statement: by measuring $R(t)$ in any of these settings, one can safely decide this question. We thank the referee for indicating minor points in the manuscript. In the resubmitted version, beyond the summary of the above ideas, we will correct those points. Once again, we sincerely thank for the report which raised fundamental questions and motivated us to think further about the applicability and testing of the proposed theory.

3 Response to Dr. Carretier

We thank our referee for a supportive review and also for raising some key issues, addressing which could substantially improve our manuscript.

Below we give a detailed, point-by-point response. also indicating changes in the resubmitted version.

Referee' comment:

At the first order, the authors could increase the impact of their findings by better relying on and linking it more closely to geological and experimental observations. The authors claim that their model "fits" the geological observations, but I see no clear evidence of such a fit in their paper. Several assertions lack references (see specific comments), in particular concerning the relative role of selective transport and attrition in the evolution of grain size along a river. In fact, selective transport has been mainly advanced to explain or model downstream fining in rivers (e.g. Paola et al., 1992; Ferguson et al., 1996; Fedele and Paola, 2007; Whittaker et al., 2011 - see list of papers at the end of this review). In parallel, several authors have shown evidence of attrition to explain the variation in grain size (e.g. Brewer and Lewin, 1993; Attal and Lave, 2006; Dingle et al., 2017). These studies are worth mentioning and discussing to show that the results presented in this manuscript are consistent with geological observations.

Our response: We agree with the referee that the list of references related to geological observations was far from complete in the original submission. In the modified manuscript we included the references suggested by the referee. We also agree with the referee that saying that our model "fits" geological observations was not a fortunate selection of expression. Certainly, as we pointed out in the main text, we did not fit the predictions of the model to any dataset - for the simple reason that currently no such dataset is available (which we discuss below). We modified the text by saying that "the model does not contradict existing geological observations."

Referee' comment:

Theoretical results could also be confronted with experimental data, which are rare and valuable. In addition to Kuenen (1956), Attal and Lavé (2009) presented pebble attrition experiments on a 1:1 scale, representing Himalayan rivers conditions. These experiments show in particular that the mass loss by attrition increases with particle velocity but is weakly dependent on particle size. As the parameter r can represent the degree of dependence between the attrition rate and the particle size, a discussion on the possible value of r in the experiments of Attal and Lavé (2009) would allow to link the theory, these experiments and the prediction of the evolution of the relative variability (focusing or dispersing) in a natural case like that of Himalayan rivers.

Our response:

Our model can be tested at two levels:

(a) at the *input level*, i.e. by testing the kernel and

(b) at the *output level*, i.e. by testing pebble size distributions.

To perform (a), one would need time evolutions for full mass distributions. We are not aware of any such publicly available dataset. To obtain such data the best options appear to be either laboratory flume or drum experiments or, in the field, radio-tagged pebble experiments.

To perform (b), one would need size dependence of abrasion rates. Such an experiment is reported in Figure 9/a of [Attal and Lavé, 2009] and we fitted our kernel to their data.

We discuss these testing options in Subsection 1.4 of the modified manuscript and we included the (b)-type kernel fit in a new Appendix (Appendix A). Here we found that the experimental data is in fair agreement with our kernel.

Referee' comment:

Statistical physics is used here in a very clever way to describe the phenomenon of attrition. However, statistical physics (and the Fokker-Planck equation) has also been used to describe the transport of grains in a river. In this case, advection-diffusion emerges from a combination of probability densities that describe the distribution of the transport distances of the particles and that of their residence time at rest (e.g. Lajeunesse et al., 2018; Nikora et al., 2002). Longer residence times for larger particles (selective sorting) may explain some of the anomalous scattering observed in tracer data (Phillips and Jerolmack, 2014; Carretier et al., 2019). In a natural system that combines both the statistical physics of transport and abrasion, how could the proposed theory be verified on the basis of field observations? What experiments or observations need to be carried out to distinguish between these two components? Again, linking this proposed theory with predictions that could be made by geologists or experimenters would increase the scope of this paper. I recommend significantly increasing the discussion in this direction.

Our response:

The relative effects of transport versus abrasion in downstream grain size evolution has been discussed in [Miller et al., 2014]. In the modified manuscript we included this reference. Direct comparison with our model could be performed, as discussed above, either at the input level (by comparing size dependence of abrasion rates) or by measuring complete time evolutions for pebble size distributions. We mention these option in Subsection 1.4. of the modified manuscript.

Referee' comment:

In the discussion, always with the aim of linking this theory with the field, I suggest discussing the following points: The pebbles impact each other but also the bedrock (which could represent a much larger volume for the population y). How would this change the result? The lateral contribution of the hillslopes modifies the initial distribution fo(x) in the real case (e.g. Attal and Lavé, 2006; Sklar et al., 2017). Can we find a natural case where the proposed theory could be tested (canyon with one particular lithology at some localized point upstream, providing tracer pebbles that could be followed downstream for example)?

Our response: We included a new subsection (Subsection 2.5) in the modified manuscript where we discuss how our model can incorporate fluvial abrasion. We show that the actual fluvial process can be bracketed by two scenarios for which our model makes the same qualitative predictions, so we may regard these predictions as valid.

Referee' comment:

The structure of this manuscript is confusing: the conclusions are described in several details in the introduction. This has the merit of setting reader's minds, but when reading it for the first time, I wondered whether it was a reminder of previous work or new findings. To guide the reader, I think it is important to write clearly what the addressed question is in the introduction.

Our response:

We appreciate the referee's comment and we re-structured the Introduction: Subsection 1.2 discusses earlier work and Subsection 1.3 summarizes our model and our results.

Specific comments

Page 2 Geological observations: extend this part based on above comments.

Done.

Page 2 Line 27-29: gives references.

Added [Huber et al., 2020].

Page 2 "as we can see": not obvious to me.

Here we only refer to the fact that in some geological settings the dominance of transport has been observed, in other settings substantial contribution from abrasion has been observed. This has been stated above and "as we can see" refers to this ambiguity.

P3 L14: "in (Domokos and Gibbons, 2013) " wrong citation format for this reference throughout the text: in Domokos and Gibbons (2013)

We used identical citation format fro all references, also for this one. On the other hand, we noticed that the bibliographical data for this paper was outdated and we corrected that error.

P4 Equation for Xt, Yt: number the equations. Give the numbers of these equations in the original paper and the corresponding notations, to help the reader.

Done.

P5 L9 Useful assumption to avoid dealing with the diffusion term in the F-P equation, but the experiments of Attal and Lavé (2009) show that fragmentation can be significant.

We agree that in energetic environments fragmentation could be significant. We considered this effect in earlier papers [Szabó et al., 2013]. However, our model is only treating the chipping phase of abrasion. To capture fragmentation, the kernel would need to be expanded and that would certainly not admit any analytical treatment. In this paper our goal was to provide a model which is capable to approximate a range of physically relevant scenarios (not all) and which, on the other hand, admits efficient analytical approximations. Further work could certainly address fragmentation by the generalization of this model.

P5 L21 "setting this is not the case": Why?

In the collective setting the size refers to the independent variable of a distribution. As the distribution evolves, parameters of the distribution evolve in time (and can be differentiated with respect to time). However, the time variation of the size x is not interpreteted in this setting.

P5 L31 "that the that the"

Done.

P6 L10: Is the correspondence with Sternberg's law demonstrated in this paper or in a previous paper?

It is demonstrated in [Domokos and Gibbons, 2018]. However, in our paper the plots in the first row of Figure 3 also show that the expected value evolves according to Sternberg's Law. This is also shown analytically in Appendix C1 for the truncated kernel.

P7 L6-10. I think it would be useful to discuss the meaning of the two populations. Are they particles of the bedload? Of the suspended load? Both? Does the collision model reflect a dynamic where the grains are in suspension? In saltation? I imagine that the physics of collisions is different in these cases.

In the modified manuscript we added Subsection 2.5 on fluvial environments where one possible geophysical interpretation of outliers is provided (the riverbed may be regarded as one single huge outlier). This does not exclude other interpretations, though.

P8 L7. Could you give a "hands-on" explanation of the nature of diffusion related to fragmentation in this case?

This line was misleading. Our model does not include diffusion but the absence of diffusion is not equivalent to prohibiting fragmentation. We altered the text in the paper accordingly.

P8 L25 Summary or summation ?
Summation. Corrected.

P8 L26-30 Explain why you are testing these other kernels whereas you announce in the introduction that the kernel finally used is "the right one".
We explained this above. We investigate the simple kernels just to show that one can NOT get away with them: while they admit analytical treatment they do not meet the most fundamental geophysical requirements. Since this is the first paper aiming to establish a statistical theory for mass evolution, we thought it would be appropriate to indicate why we do not use any of the simple kernels. On the other hand, more complicated kernels may be closer to the physics of the process but would be, most likely, beyond the reach of analysis.

We describe that our choice for the kernel is a trade-off between physical accuracy and mathematical transparency.

P9 L12: Proportional TO projected ? (could you give a reference?)

Corrected. Appendix D added.

P9 L21-27 Give references or explain better the values deduced for r. Again, do these r values depend on the type of transport (suspension, saltation etc.)?
The estimates on the parameter r are now better explained in Appendix D.

P9 L 26-27 Important to make the link with the field. Expand on this aspect.
We added Appendix D to explain the values of r. On the other hand, making specific predictions for field data appears to be a bit far-fetched at this stage. We do believe that r is characteristic of the environment. The fitting of the kernel to the data of Attal and Lavé in Appendix A shows that energetic fluvial environments correspond to low values of r, as we indicated. We do not have other data currently.

P9 L32 what is V? (Volume I think but I have not seen its definition above).
Corrected. It should have been X (not V).

P11 L10 justify why you take a log-normal law for fo. Does the result change if you take another law?
We took a lognormal distribution because most mass distributions can be well approximated by this. None of the qualitative features of the model are influenced by the particular type of the distribution.

P11 L11: "The applied time step is fixed at Δt = 0.01." Already said above.
Corrected (removed).

P11 Figure 4: Indicate c: continuous and d: discrete in the caption. Because the by-product of abrasion is removed, I would have expected that the distribution tends toward a Dirac at x=0 in all the cases. Why is it not the case? ("hands-on" explanation please;). In the focusing case, what determines the final x value of the Dirac?

"c" and "d" added to caption.

The referee is right, in the focusing case the distribution converges onto the x=0 Dirac Delta. In our plots we followed the evolution only for finite time (t=5) so we see a very sharp peak in the vicinity of 0.

P12-12 3.3 Very interesting discussion. In Figure 4 it could also be argued that the tail of the distribution between 2E-7 and 2E-6 is a power law, while the outliers represent a subsampling of the actual distribution, as often observed in seismology (for magnitude) or hydrology (for peak discharge). Could the persistence of these outliers indicate some fractional derivative component not taken into account in the Fokker Planck equation?

A very interesting point. The Fokker-Planck equation in eq. (7) in the paper indeed resembles a problem with a spatial fractional derivative. It might be argued that a kernel could be selected such way that one of the widely used fractional derivatives formulas (such as the Caputo fractional derivative) is retrieved. However, to the best of our knowledge, the compound kernel in the paper does not establish any known fractional derivative formula. But this does not contradict the observation of the reviewer: we think that although the outliers are identified in finite samples of N particles, the result in Appendix E is based on the $N \to \infty$ limit. This implies that a well-chosen bimodal distribution (with a small peak representing the outliers) would also predict the survival of the outliers, and this is also suggested in Figure 7. We think that although our model formally does not contain a fractional derivative, the behaviour of the tail of the distribution is very similar to models with an established fractional derivative.

P14 "(a) existing geological observations": not demonstrated in my opinion.

We added Subsection 1.4 about the two possible levels of testing our model and demonstrated in Appendix A that the model exhibits reasonable agreement with experimental data.

References

[Attal and Lavé, 2009] Attal, M. and Lavé, J. (2009). Pebble abrasion during fluvial transport: Experimental results and implications for the evolution of the sediment load along rivers. *Journal of Geophysical Research: Earth Surface*, 114(F4).

[Domokos and Gibbons, 2018] Domokos, G. and Gibbons, G. W. (2018). The geometry of abrasion. In Ambrus, G., Bárány, I., Böröczky, K. J., Fejes Tóth, G., and Pach, J., editors, *New Trends in Intuitive Geometry*, pages 125–153. Springer Berlin Heidelberg, Berlin, Heidelberg.

[Huber et al., 2020] Huber, M. L., Lupker, M., Gallen, S. F., Christl, M., and Gajurel, A. P. (2020). Timing of exotic, far-traveled boulder emplacement and paleo-outburst flooding in the central himalayas. *Earth Surface Dynamics*, 8(3):769–787.

[Miller et al., 2014] Miller, K. L., Szabó, T., Jerolmack, D. J., and Domokos, G. (2014). Quantifying the significance of abrasion and selective transport for downstream fluvial grain size evolution. *Journal of Geophysical Research: Earth Surface*, 119(11):2412–2429.

[Szabó et al., 2013] Szabó, T., Fityus, S., and Domokos, G. (2013). Abrasion model of downstream changes in grain shape and size along the williams river, australia. *Journal of Geophysical Research: Earth Surface*, 118(4):2059–2071.

[Uberoi, 1957] Uberoi, M. S. (1957). Equipartition of energy and local isotropy in turbulent flows. *Journal of Applied Physics*, 28(10):1165–1170.

Particle size dynamics in abrading pebble populations

András A. Sipos[1,2], Gábor Domokos[1,2], and János Török[1,3]

[1] MTA-BME Morphodynamics Research Group Budapest University of Technology and Economics, Műegyetem rakpart 1-3, Budapest, Hungary

[2]Department of Materials and Structures, Budapest University of Technology and Economics, Műegyetem rakpart 1-3, Budapest, Hungary

[3]Department of Theoretical Physics, Budapest University of Technology and Economics, Budafoki út 8, Budapest, Hungary

Correspondence: András A. Sipos (siposa@eik.bme.hu)

Abstract. Abrasion of sedimentary particles in fluvial and aeolian environments is widely associated with collisions encountered by the particle. Although the physics of abrasion is complex, purely geometric models recover the course of mass and shape evolution of individual particles in low and middle energy environments (in the absence of fragmentation) remarkably well. In this paper, utilizing results of this individual, geometric abrasion theory as a *collision kernel*, following techniques adopted in the statistical theory of coagulation and fragmentation, we construct the corresponding Fokker-Planck equation as the first model for the collision-driven *collective* mass evolution of sedimentary particles. Our model uncovers a startling fundamental feature of collective particle size dynamics: collisional abrasion may, depending on the energy level, either focus size distributions, thus enhancing the effects of size selective transport or it may act in the opposite direction by dispersing the distribution. This complex behaviour does not contradict existing geological observations on mass distributions.

1 Introduction

1.1 Geological observations

Probably the most fundamental observation on pebbles is that they appear to be segregated both by size and shape and it is broadly accepted that the dynamics is driven by two physical processes: transport and abrasion. Which of these processes dominates may depend on the geological location and also on timescales, however, geologists appear to agree that, in general, neither process should be ignored.

In *coastal environments,* one of the most remarkable accounts of pebble size and shape distribution is provided by Carr (Carr, 1969) based on the measurement of approximately a hundred thousand pebbles on Chesil Beach, Dorset, England. In summarizing his results, Carr provides mean values and sample variations for maximal pebble size and pebble axis ratios along lines orthogonal to the beach. These plots reveal pronounced segregation by maximal size and shape, i.e. on shingle beaches pebbles of roughly similar maximal sizes and with roughly similar axis ratios appear to be spatially close to each other. Size and shape segregation has been broadly observed in various settings (Bird, 1996; Gleason et al., 1975; Hansom and Moore, 1981; Kuenen and Migliorini, 1950; Neate, 1967) and it was mostly attributed to the global transport of pebbles by waves (Lewis, 1931; Carr, 1969) but, in some settings, may also be related to abrasion. Indeed, a detailed account of the interaction of abrasion and transport is given by Landon (Landon, 1930) who investigated the beaches on the west shore of Lake Michigan. He attributes size and shape variation to a mixture of abrasion and transport. Kuenen (Kuenen, 1964) discusses Landon's observations, however disagrees with the conclusions and attributes size and shape variation primarily to transport. Carr (Carr, 1969) observes dominant sizes and shape ratios emerging as a result of abrasion and size grading while Bluck (Bluck, 1967) describes beaches in South Wales where equilibrium distributions of size and shape are reached primarily by transport and abrasion plays a minor role. Which of the two processes (transport or abrasion) dominate may well depend on the timescales they operate on. While abrasion appears in some scenarios to act much slower than transport, a recent study (Bertoni et al., 2016) verified mass losses on the order of 50% on a pebble beach over a 13-months period, indicating that in some settings the two processes may indeed compete in determining size and shape distributions.

In *fluvial environments*, while downstream fining of sediment has been often attributed to transport Paola et al. (1992); Ferguson et al. (1996); Fedele and Paola (2007); Whittaker et al. (2011), other authors have pointed to the significance of attrition Brewer and Lewin (1993); Attal and Lavé (2006); Dingle et al. (2017). In Miller et al. (2014) the authors, using field data, provide quantitative assessment of the significance selective transport with respect to attrition in downstream fining. Beyond the evolution of smooth size and shape distributions, there is yet another common phenomenon in fluvial geomorphology where the interaction of transport and attrition could be far from trivial. The often observed presence of isolated large boulders in rivers Huber et al. (2020) may be explained solely by transport, as these large pieces are often not carried by the river, rather, they move by a different process (e.g. landslide or debris flow). On the other hand, these large rocks could also be interpreted as *outliers* emerging spontaneously in a pebble size distribution on which collisional abrasion certainly has strong impact in upper reaches of rivers.

As we can see, both in coastal and fluvial environments it is a generally accepted fact that the two processes (transport an attrition) appear to *compete* in shaping the evolution of pebble shape and pebble mass distributions. How exactly this competition may play out and in what manner attrition may contribute to this process is the subject of our paper.

We also remark that while all available observations indicate that attrition could be a relevant factor in the evolution of shape and mass distributions, so far, in the absence of any predictive theory, no datasets have been collected which would admit to verify any theoretical predictions. We will point out potential strategies for verification in Section 4.

1.2 Existing theory

1.2.1 Individual abrasion

Individual abrasion is a theory describing the mass and shape evolution of one individual particle (*abraded particle*) under the impacts of many incoming particles (*abraders*) (see Figure 1(a)). In the mean field theory for the geometry of individual abrasion only the mass and shape of the abraded particle is recorded, the effect of impacts is averaged and the evolution is determined by the size of the abraded particle compared to the average size of the abrading particles.

The mean field geometric theory of individual abrasion (i.e. shape evolution) for sedimentary particles under collisions is, since the seminal papers by Firey (Firey, 1974) and Bloore (Bloore, 1977), well understood and validated (Szabó et al., 2013; Szabó et al., 2015; Novák-Szabó et al., 2018). Still, despite the success of the Firey-Bloore geometric theory of shape evolution it was clear (Domokos and Gibbons, 2018) that it is not suited to predict the evolution of size: in stark contrast with geological observations summarized in Sternberg's Law (Sternberg, 1875), predicting exponential decay of particle mass and *infinite lifetime* for all particles, geometric abrasion theory predicted *finite lifetime* for all particles. On the other hand, Sternberg's broadly accepted theory of mass evolution (Sternberg, 1875) had nothing to offer regarding the evolution of shape. Recognizing this challenge, in (Domokos and Gibbons, 2018) a unified theory, called *volume weighted shape evolution* has been proposed which, on one hand, reproduces all the geometric features of the Firey-Bloore geometric theory, on the other hand, it also predicts mass evolution in accordance with Sternberg's Law.

1.2.2 Binary abrasion

The first stepping stone between the theory of individual abrasion and collective abrasion is the model for *mutual, binary* abrasion where two particles mutually abrade each other and we track both evolutions (see Figure 1(b)). In this case one can still write mean field equations by averaging over many collisions and the mass and shape evolution of both particles are recorded. For any binary abrasion model of size evolution, we postulate the following requirements:

- size evolution should follow Sternberg's Law,
- mass loss in a collision should be a monotonically increasing function of collision energy and
- the model should be fully compatible with the geometric evolution model.

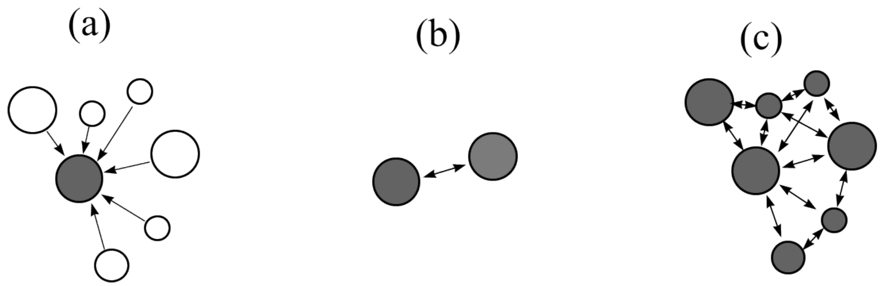

Figure 1. Schemes for (a) individual abrasion, (b) binary abrasion and (c) collective abrasion, respectively. Volume loss only tracked for shaded particles. Arrows represent (non-simultaneous) collision events between particles.

The unified theory in (Domokos and Gibbons, 2018) offers a model satisfying all three requirements: by extending the Firey-Bloore equations and Sternberg's theory and using the kinetic energy of collision, models for *binary shape evolution* and for *binary mass evolution* of two mutually abrading particles were put forward. These two models have been merged in (Domokos and Gibbons, 2018) into a unified volume weighted theory of binary abrasion, compatible both with the Firey-Bloore and with the Sternberg theory. The volume weighted model for binary mass evolution, describing the time evolutions for the masses $X(t), Y(t)$ of two particles with respective material properties m_1, m_2 can be written as

$$X_t = -c_{12}\frac{XY}{X+Y}, \tag{1}$$

$$Y_t = -c_{21}\frac{YX}{X+Y}, \tag{2}$$

where the subscript t refers to differentiation with respect to time and the constant prefactors c_{12} and c_{21}, which we call the *binary abrasion parameters*, depend simultaneously on the materials m_1 and m_2 of the X and Y-particles, respectively.

We also note that in case of two *indentical* particles (e.g. two particles with identical masses $X = Y$ and identical material properties $c_{XY} = c_{YX}$) the system (1) and (2) predicts mass evolution according to Sternberg's Law. In case of different masses or properties we still have infinite lifetime with one of the particles approaching zero mass asymptotically as times goes to infinity and the other particle approaching a finite mass.

1.2.3 Collective size dynamics

Independently of individual (and binary) abrasion theory there exists broad interest in *collective* shape and size evolution models tracking mutually colliding populations of N particles (see Figure 1(c)). Similar problems arise in particular in the context of coagulation (da Costa, 2015) and dynamic fragmentation processes (Cheng and Redner, 1988). In such collective evolution models the main question is how the size distribution of particles, starting from an initial distribution, evolves in time due to the mutual collisions. These models use a standard framework relying on a so-called *collision kernel*. In a more general setting, the collision kernel is referred to as the *interaction kernel*. Our choice of terminology is motivated by the fact that in our case the only interactions are collisions.

The collision kernel can be derived from the binary equations (the physical model of the $N = 2$ case) by incorporating statistical effects, i.e. that collision probability may depend on particle speed or mass. In (Domokos and Gibbons, 2018) the binary model (1) and (2) was extended to a kernel by introducing an additional scalar parameter r (to which we will also refer to as the *environmental parameter* of the evolution), representing the assumption that on the average, only the collision probability depends on particle size and the collision speed is independent of mass:

$$X_t = -c_{12}\frac{X^{1+r}Y^{1-r}}{X+Y}, \tag{3}$$

$$Y_t = -c_{21}\frac{Y^{1+r}X^{1-r}}{X+Y}. \tag{4}$$

Note that these equations are identical to the formulas (118) and (119) in (Domokos and Gibbons, 2018) with $\alpha = 0$ in their notation and taking $r = \nu$, $X = V_X$, $Y = V_Y$, $c_{12} = c_{21} = c$. Alternative interpretations of r are also possible; we will discuss the role of the environmental parameter r in detail in Subsection 2.4. Henceforth, in the main body of this paper (apart from Appendix A) we assume that the pebble population is *homogeneous*, i.e. that the material for all pebbles is identical so we have $c = c_{12} = c_{21}$ and the sole role of the constant c is to set the timescales. We will incorporate this into the time variable t and henceforth, for homogeneous pebble populations, we set $c \equiv 1$. We will discuss the role and identification of material constants in heterogeneous pebble populations in Appendix A.

Once the kernel has been established, we make the assumption that for large N the collective size evolution is a stochastic process driven by many binary events among the particles, implying that the core of the collective process is still the above mentioned collision kernel. This allows for the construction of the *master equation*, also known as the Fokker-Planck equation which describes the time evolution of the particle size distribution. Although the collective abrasion is a stochastic process, in the $N \to \infty$ limit the collision kernel will uniquely determine the global evolution of the continuous size distribution. The master equation (or Fokker-Planck equation) is expressing this evolution. Determining the master equation based on the collision kernel is the second step in the statistical model.

1.3 Our model

1.3.1 Relationship to earlier models

The above-outlined structure is characteristic for *coagulation fragmentation* models (da Costa, 2015), in particular for non-linear fragmentation, which describe fragmentation processes triggered by binary collisions of particles. Our model may be regarded as a special case of the non-linear fragmentation models (Cheng and Redner, 1988) since, in addition to the standard framework adopted in these models we also make two simplifying assumptions:

1. we only consider collisions where the relative mass loss is small (i.e. the particles lose only fragments with small relative mass) and
2. the small fragments generated in the collisions are not considered further in the evolution.

By implementing these two assumptions into the statistical model based on the collision kernel (3) and (4), we take the first step towards establishing the statistical theory of collective size and shape evolution of sedimentary particles. This approach offers multiple methodological advantages. On one hand, by using (4) as the collision kernel, our statistical model will be compatible with Sternberg's Law so we can expect the collective evolution also to observe this theory, albeit in a statistical sense. On the other hand, we can also expect all our results to be compatible with an extended (future) theory which also describes collective shape evolution based on the unified, volume weighted geometric theory in (Domokos and Gibbons, 2018).

1.3.2 Basic notations

To describe our construction we will need to address both the size evolution of individual particles (under the collision kernel) as well as the evolution of size distributions. While particle size appears in both settings, we need to distinguish carefully: in individual and binary models particle size evolves in time, in collective models size distribution evolves in time. As a consequence, in the individual setting the variable denoting size may be differentiated with respect of time, in the collective setting this is not the case. We will use X,Y to denote individual particle sizes (either volume or mass) and we will use x,y to denote the independent variables of size distributions. Time evolution of individual particle size will be denoted by $X(t),Y(t)$ with time derivatives $X_t(t),Y_t(t)$ (subscript will refer to differentiation throughout the paper). The time evolution of size densities will be denoted by $f(x,t),f(y,t)$ with time derivatives $f_t(x,t),f_t(y,t)$ and size-derivatives $f_x(x,t),f_y(y,t)$. We denote the expected value and variance of these size distributions respectively by $E(t)$ and $W(t)$ and we will primarily use the relative variance $R(t)=W(t)/E(t)^2$ to characterize the evolution of the distributions.

1.3.3 Main results

The collision kernel (3) and (4) for mass evolution in (Domokos and Gibbons, 2018) has one single environmental parameter r which is inherited by the corresponding Fokker-Planck equation (shown in Subsection 2.2). As we will describe in Section 2, the environmental parameter r may, depending on interpretation, represent either the size dependence of the number of collisions or, alternatively, the size dependence of collision energy. Regardless of the interpretation, in Subsection 2.3 we find that the value $r=0.5$ is *critical* as it separates two regimes of collective abrasion with qualitatively different evolution $R(t)$ of the relative variance :

- For $r>0.5$ we find *focusing* processes with decreasing $R(t)$, approaching $R(t)=0$ in the limit as time approaches infinity. Here the size distribution converges to a Dirac delta function. This parameter range corresponds to lower energy levels. Natural abrasion processes belonging to this regime will thus amplify the segregating effects of size-selective transport.

- For $r<0.5$ we find *dispersing* processes with increasing $R(t)$, thus counter-acting size-selective transport processes. This corresponds to collisional abrasion at higher energy levels.

As collisional abrasion may occur at a broad range of energies, these two basic scenarios of the model (illustrated in Figure 2) offer an explanation for the broad range of geological observations (Bluck, 1967; Landon, 1930; Carr, 1969; Kuenen, 1964)

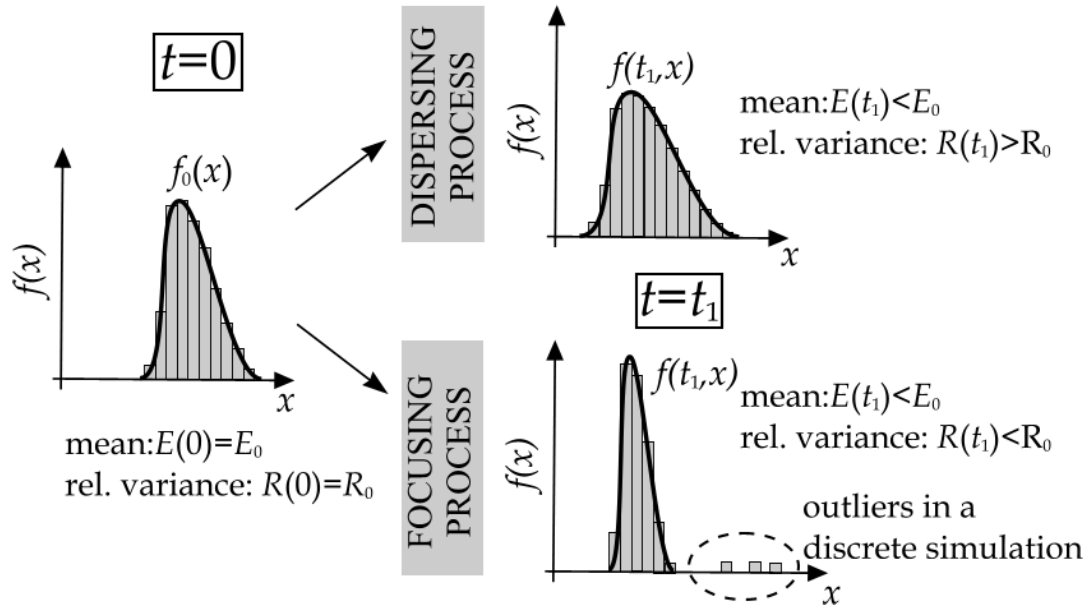

Figure 2. Schematic description of the evolution of mass distribution of a pebble population: in a dispersing process the $R(t)$ relative size variation of the a mass distribution, either represented by an empirical histogram (Carr, 1969), or a continuous function ($f_0(x)$) at $t=0$, is increasing. In a continuous focusing process $R(t)$ decreases as time evolves, however, in a discrete setting some outliers (indicated by dashed ellipse) with mass substantially above the average. The reduced distribution (without the outliers) produces a decreasing relative variance, analogous to the continuous model.

in relating the relative significance of transport and abrasion in various scenarios. Our model also reflects the universality of Sternberg's Law by predicting, regardless of the environmental parameter r, exponential decay as the universal evolution $E(t)$ of the expected value.

In general, the evolution equations generated by (3) and (4) for the mean $E(t)$ and the variance $W(t)$ are integro-differential equations which are hard to solve analytically. To support our claims, we will use three types of approximations:

(a) We approximate the kernel (3)-(4) by its truncated Taylor series expansion and investigate the evolution of general initial density functions. This is found in Appendix C1.

(b) We regard the full kernel, however, we only investigate density function obtained as a small perturbation of the Dirac delta (i.e. populations of *almost* identical particles). This is done in Appendices C2 and C3.

(c) We numerically compute both the discrete and the continuum models. For details see Section 3.

We will briefly refer to the first two approximations as the *continuum model*. In case of the third approximation we do direct, discrete simulations of finite particle populations we use the full kernel and we call this the *discrete model*. One startling feature of the latter (as compared with the former) is the appearance of *outliers*, i.e. particles substantially larger than the vast majority (illustrated in Figure 2). As we can observe, the bulk of the density function closely mimics the evolution in the continuum model. The quantitative analogy in the evolution of the relative variation R can be also recovered if we consider a reduced density function $f^\star(t_1,x)$ by omitting the outliers, i.e by applying an upper cutoff in size, omitting bins containing only one particle. The reduced density function $f^\star(t_1,x)$ is characterized by the reduced relative variation $R^\star$ which will decrease in a focusing process, however, in contrast to the continuum model, it will not approach zero, rather a positive constant.

1.4 Testing of the model for homogeneous pebble populations

As outlined above, our model is defined on two levels: the collision kernel (3)-(4) we will briefly refer to as the *input level* as it defines the basic physics of the underlying collisions. The Fokker-Planck equation we will briefly refer to as the *output level* as it defines the evolution of the mass density function based on the collision kernel. One may test the model at both levels. Below we discuss the case of homogeneous pebble populations where the evolution of the mass distribution is controlled by the single material parameter c and the single environmental parameter r:

(a) One may test the model at the *input level*, by fitting the kernel (3)-(4) to laboratory tests where abrasion rate is plotted as a function of particle size. Such an experiment could be used to determine the material parameter c for a given homogeneous population. Also, if the laboratory test is imitating the environment of the natural process, the environmental parameter r may be also obtained in this manner. We also note that the functional relationship between particle size and abrasion rate will not only depend on the parameters but also on particle size. For details, see Appendix A.

(b) One may test the model at the *output level* by measuring the time evolution of full mass distributions and fitting the respective material and environmental parameters c and r to this dataset. While we are not aware of any such public dataset, this could be performed in a laboratory either in a flume or in a drum experiment. In the field the optimal solution appear to be radio-tagged pebbles (Bertoni et al., 2016).

The above simple procedures apply only for homogeneous populations. We lay out the procedures for the testing of the model for heterogeneous populations in Appendix A where we also perform partial testing for the laboratory data obtained by (Attal and Lavé, 2009).

2 Modeling collective size dynamics

2.1 General form of the collision kernel

The first simplification described in Subsection 1.3.1 implies that the limit where relative fragment mass approaches zero offers a good approximation, thus it admits a collision kernel of the type used in Ernst and Pagonabarraga (2007), describing continuous mass evolution via coupled ordinary differential equations for the evolution of particles with masses $X(t)$ and $Y(t)$:

$$-X_t = \psi^1(X,Y), \tag{5}$$

$$-Y_t = \psi^2(X,Y), \tag{6}$$

where $\psi^1(X,Y)$ and $\psi^2(X,Y)$ are differentiable (C^1) functions, with positive values (i.e. $\mathbb{R}^+ \times \mathbb{R}^+ \to \mathbb{R}^+$). Symmetry of the binary process implies $\psi^1(X,Y) = \psi^2(Y,X)$, so often superscripts are suppressed and the kernel is simply referred to as $\psi(.,.)$. Selection of the kernel encapsulates not only the physics of binary collisions, it also may include the mass-dependent probability of collision between two particles. We will discuss the identification of a physically sound kernels in Subsection 2.3.

2.2 General form of the master equation

The second simplification in Subsection 1.3.1 admits the construction of the master equation solely based on the collision kernel (by omitting additional terms for the remainder of the fragmented material). These simplifying assumptions also set our model apart from general fragmentation models in another respect: in the latter, constant mass is prescribed as a global time-invariant while the (integer) number of particles changes whereas in our model total mass is decreasing while the number of particles remains constant and serves as a global invariant.

Using these considerations, for our problem the master equation is found to be

$$f_t(t,x) = \frac{\partial}{\partial x}\left[f(t,x) \int_0^\infty f(t,y)\psi(x,y)dy \right] = f_x(t,x)\int_0^\infty f(t,y)\psi(x,y)dy + f(t,x)\int_0^\infty f(t,y)\psi_x(x,y)dy, \tag{7}$$

where subscripts stand for partial derivatives. Without loss of generality, the evolution starts at $t=0$ and we consider the initial distribution of the volume $f(0,x) \equiv f_0(x)$ to be *a-priori* known. Note that contrary to the majority of Fokker-Planck models, our model contains solely the advection term, which readily follows from the deterministic nature of the kernel. Here we aim to figure out the collective behavior implied by (7). Nonetheless, a stochastic kernel would produce diffusion in the master equation, such a generalization might be essential for testing model predictions against experimental data.

We aim to understand some scenarios characteristic of pebble populations by investigating the Cauchy-type initial value problem associated with equation (7), starting at the distribution f_0 with mean value E_0, variance W_0 and relative variance $R_0 := W_0/E_0^2$.

2.3 Collision kernels

Detailed physical modeling of the collisional event can make the interaction kernel highly complex; for a recent review on kernels see (Meyer and Deglon, 2011). On the other hand, mathematical studies tend to prefer simple expressions for $\psi(X,Y)$, admitting rigorous, analytical conclusions. Our goal is to a find kernel which has strong physical basis, yet it admits an analytical approach, thus it offers a trade-off between between physical and mathematical preferences.

We first consider two simple kernels which satisfy the mathematical requirement of leading to analytically soluble Fokker-Planck equations. However, as we will show, these very analytical results highlight that these kernels are physically not admissible. Next, we investigate the parameter dependent compound kernel suggested in (Domokos and Gibbons, 2018) which grabs the essential physics of the investigated process, yet, the corresponding Fokker-Planck equation still admits analytical conclusions.

First, we consider the *summation kernel* (denoted by $\{.\}^+$), where the mass loss rate is proportional to the sum of the masses of the colliding particles:

$$\psi^+(X,Y) := X + Y, \tag{8}$$

stating that the rate of mass loss in binary collisions is proportional to the total mass of the two colliding particles. Appendix B1 demonstrates that the relative variance of the mass in case of the summation kernel follows $R^+(t) = R_0 e^{2t}$, hence it is a *dispersive* process regardless of the initial distribution f_0.

In the very same manner let us investigate the *product kernel* distinguished by the sign $\{.\}^*$. The product kernel is defined via

$$\psi^*(X,Y) := XY. \tag{9}$$

According to Appendix B2, the relative variance in this case is constant as $R^*(t) = R_0$ for all $t \geq 0$, which that the model is nor focusing neither dispersing. Note that the time-invariance of $R^*(t)$ under the product kernel does not imply the invariance of the P.D.F $f(t,x)$ per-se. In addition, we see a polynomial decay in the mass as $E^*(t) = (t + E_0^{-1})^{-1}$, which contradicts Sternberg's law (Sternberg, 1875) that postulates an exponential decay.

In order to be in accordance with Sternberg's law and to have a control on the evolution of the relative variance, following the lead of (Domokos and Gibbons, 2018) we investigate the interaction law (3) and (4) which we call a *compound kernel* and using the introduced general notation for kernels, we distinguish it with the $\{.\}^c$ sign:

$$\psi^c(X,Y) := \frac{X^{1+r} Y^{1-r}}{X+Y}, \tag{10}$$

where $0 \leq r \leq 1$ is a fixed parameter. Henceforth we investigate evolution of mass density functions under the Fokker-Planck equation derived from (10). In Appendix C1 we show analytical results for the evolution if the kernel (10) is replaced by its truncated Taylor expansion. In Appendices C2 and C3 we show analytical results for the evolution under (10), using a Dirac delta as initial distribution. The evolution under (10) with no restrictions for the initial condition is studied numerically. The essential properties of the three investigated kernels are summarized in Figure 3.

2.4 Interpretation of the parameter r

In natural events, both velocity and collision probability (cross-section) may depend on particle size: in laminar flows relative velocity and collision probability is proportional to linear size, while in a turbulent flows velocity could be inversely proportional to linear size and collision probability could be proportional to projected area. In the collision kernel (10) both effects (dependence of velocity and dependence of collision probability on speed) are represented by the single scalar parameter r, so one may freely assign various interpretations to this parameter. In Domokos and Gibbons (2018) one particular interpretation was used: the compound kernel was derived using the assumption that particle velocity is independent of the size (e.g. rather determined by the surrounding fluid), but the collision probability goes as a power law with particle size, i.e. X^r. The effective mass combined with the collision probability gives the kernel in Eq. (10). However, alternative interpretations are possible,

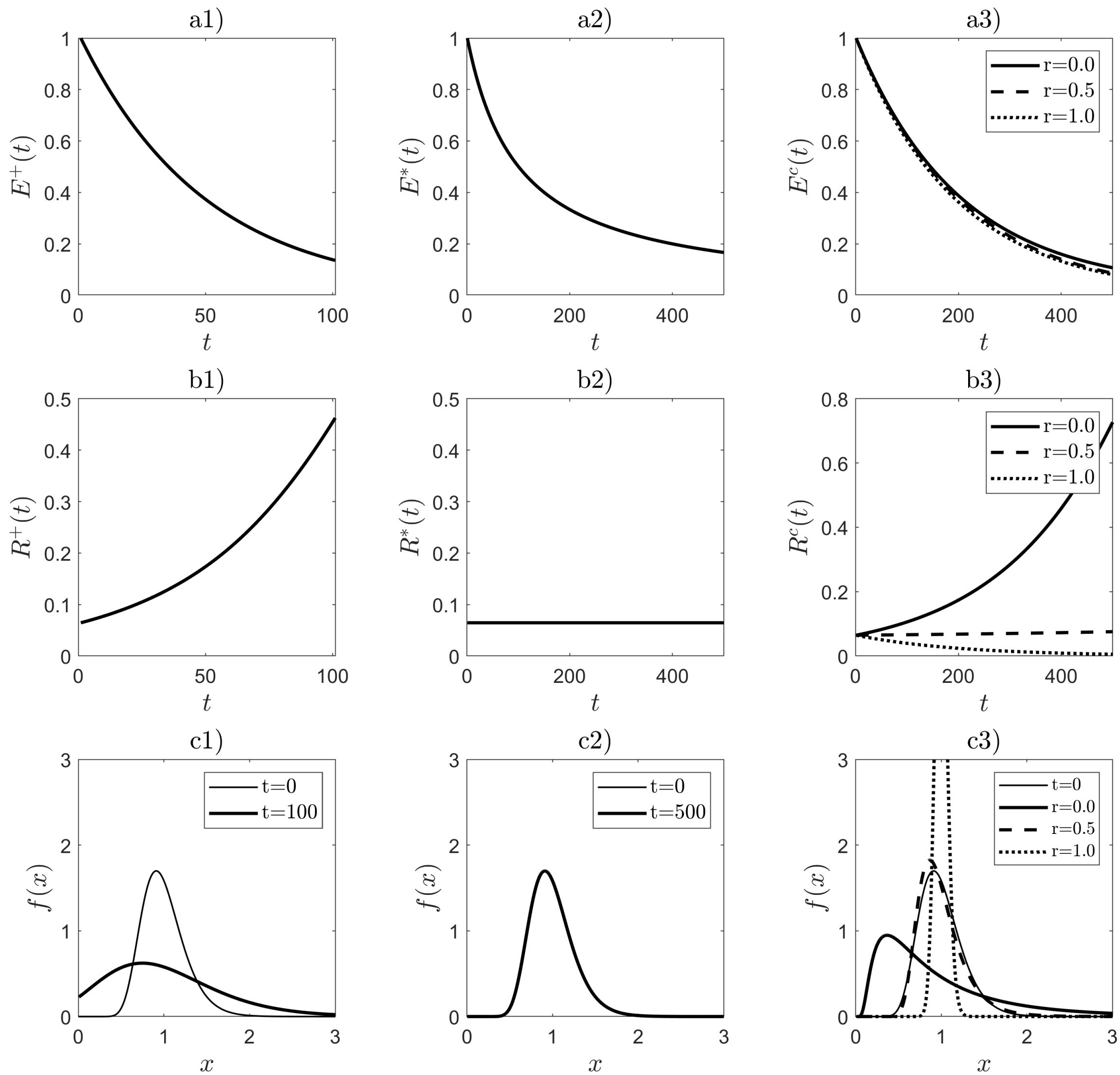

Figure 3. Evolution of an initial ($t = 0$) lognormal probability density function under Fokker-Planck equation generated by various kernels. Summation kernel: a1,b1,c1. Product kernel: a2,b2,c2. Compound kernel:a3,b3,c3. First row (a1,a2,a3): mean $E(t)$. Second row (b1,b2,b3): relative variance $R(t)$. Third row (c1,c2,c3): initial ($t = 0$) and final densities $f(x,t)$.

the only essential underlying assumption is that we regard a one-parameter family of scenarios. In this family, if velocity is proportional to X^a and collision probability is proportional to X^b then we have $r \simeq a + b$.

To have a global view, it may be of interest to estimate the parameter r in two extreme (limiting) scenarios. Laminar flows are characterized by a linear velocity profile. The particles hit each other if their trajectories intersect. Integration of the linear velocity profile combined with a spherical particle shape yields a collision probability proportional to $\sim X^{2/3}$ or, alternatively

$r \simeq 2/3$. The other extreme case corresponds to turbulent flows, where we have *equipartition*, i.e. the kinetic energy of the particles is independent of their size (see e.g. Uberoi (1957)), implying that particle velocity is proportional to $X^{-1/2}$. Since the area of the cross-section is proportional to $X^{2/3}$ we arrive at a collision probability $X^{1/6}$, or, alternatively $r \simeq 1/6$. As we can see, both extreme scenarios yield r values far away to either side of the critical value $r_{\text{crit}} = 1/2$, so these estimates suggest that smooth steady conditions should result in a focusing and turbulent gas-like behavior in a dispersing process. For a detailed derivation see Appendix D.

In order to examine the validity of these assumptions we made discrete element simulations using the event driven method Lubachevsky (1991). In event driven dynamics, collisions are considered instantaneous and resolved accordingly which is best suited to obtain proper collision statistics. We emulated the above-mentioned processes by choosing an artificial mass for the particles and simulating a chaotic system. The artificial mass was used to obtain different volume-velocity relations in different scenarios. We found that in chaotic/turbulent systems that relative velocities were proportional to $v \sim X^{-1/2} – X^{-1/3}$ and the system behaved as the continuum model with $r \sim 1/6 - 1/3$. On the other hand, if velocities were proportional to $v \sim X^{-1/6} – X^{0}$ then the system was similar to a continuum model with $r = 1/2 - 2/3$. Thus the discrete element simulations fully support the results of the compound kernel.

2.5 Fluvial abrasion

Here we interpret the intuitive picture of fluvial abrasion in the context of our statistical model. In our model a fluvial environment may be represented by a *fluvial population*, consisting of $N + 1$ particles: a very large number (N) of small particles X^i ($i = 1, 2, \dots N$) representing the pebbles carried by the river and one very large particle Y representing the riverbed. Such a scenario can not be explored directly in the context of our continuum model, however, as we will discuss in detail in Subsection 3.3, the discrete model can capture this situation even in the limit as $N \to \infty$.

To make a meaningful characterization of geologically relevant scenarios, we will regard two extreme cases which represent brackets on geological processes. In both cases we assume that the mass evolution is driven by binary collisions and we regard the limit as $N, Y \to \infty$ (while the masses X^i of the small particles remain finite). Since we are interested in the mass evolution of pebbles (and in the current paper we are not interested in the mass evolution of the riverbed) we will denote the relative variance of the pebble population (i.e. all X^i particles, the riverbed Y not included) by $R(t)$. Our aim is to establish the sign of $R_t(t)$ as the main qualitative feature of collective dynamics.

In the first extreme scenario we assume that particles are chosen uniformly from the full *fluvial population*: i.e., the riverbed has no special role. In this case *almost all* collisions will happen among a pair of small particles (X^i, X^j) thus the presence of the riverbed has no impact on the evolution of $R(t)$. For this extreme case all predictions of our continuum model remain valid: $r = 0.5$ will be a critical parameter value above which we see focusing ($R_t < 0$), below which we see dispersing ($R_t > 0$) behaviour. At the critical value $r = 0.5$ our model predicts neutral behaviour with $R_t = 0$.

In the second extreme scenario we assume that the small particles *exclusively* collide with the riverbed (large particle), i.e., we only have (X^i, Y)-type collisions. This means that the evolution for each of the small particles is an identical, independent two-particle process governed by the model (1)-(2) for binary collisional mass evolution. In this process, in the $Y \to \infty$ limit each individual small particle X^i will thus evolve as

$$X^i(t) = X^i(0)e^{-t} \tag{11}$$

and thus follow Sternberg's Law. It is easy to show that for any initial distribution for the masses $X^i(0)$, in this process we have $R_t = 0$. The large Y-particle (riverbed) will lose some mass as well but in this publication we are not interested in that part of the process.

Intuitively it is clear that any geologically relevant process is in-between the above two extreme cases and, although we do not deliver a rigorous proof, it appears plausible that in a geologically relevant setting R_t will be also bounded by the two evolutions predicted for the two extreme scenarios. As for the second extreme scenario we have $R_t = 0$ we expect that for any intermediate scenario the sign of R_t will agree with the sign of R_t based on the first extreme scenario. This would imply that all our qualitative predictions remain valid in fluvial environments.

3 Numerical results

Here we perform computations to illustrate the main results presented in Subsection 1.3.3 by discretizing time with a fixed time-step Δt. The discrete model has been simulated with custom-made codes in Matlab and Python performing $M * [N/2]$ collisions between pairs during one time-step Δt, where M is fixed model parameter and N is the size of the population. The simulation starts with the creation of N particles whose volumes are randomly sampled from the initial distribution f_0. Binary collisions are performed on uniformly selected pairs, i.e., all particles have equal chance of being selected irrespective of their volume. Once a pair is selected, the collision kernel ψ^c is applied and volume decrement is computed with time-step $\Delta t/M$. After the binary collision event both particles with reduced volume are replaced into the sample. In the presented simulations we set the population size to be $N = 5000$, the time-step $\Delta t = 0.01$ and $M = 10$. In the continuum setting $f(t,x)$ evolves under eq. (7) with some initial value $f_0(x)$. This code uses the operator exponential syntax of a the Chebfun toolbox (Driscoll et al., 2014) in Matlab.

3.1 Focusing and dispersing regimes

The evolution of a pebble population under the compound kernel was simulated both in the frame of discrete and the continuum model, i.e. by direct event-base simulation and by discretizing the partial differential equation. (see Sec. 1.3.3). The results show excellent agreement with our analytical predictions: $r = 1/2$ appears indeed a critical parameter in the model. This is illustrated in Figure 4 where a lognormal distribution is used as an initial value for the evolution.

3.2 Fitted lognormal distribution

Although the lognormal distribution is certainly *not* invariant under the compound kernel (i.e. an initially lognormal density function does not remain lognormal in the evolution), however, mass distributions in later timesteps highly resemble lognormal dsitributions. To test this visual observation we fitted lognormal distributions to the computed mass distributions in the discrete

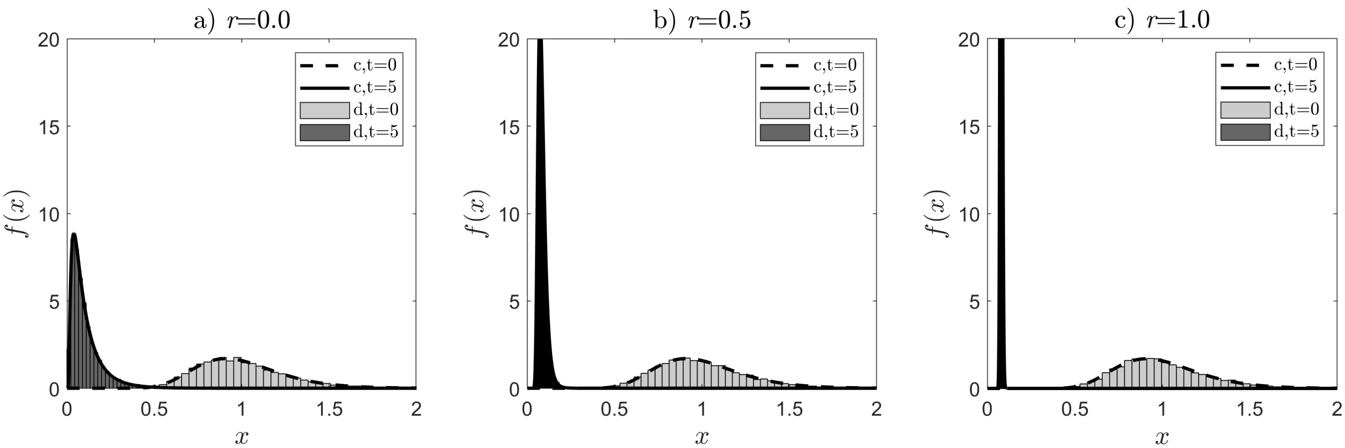

Figure 4. Evolution of a lognormal P.D.F in the compound kernel under the continuous (c) and discrete (d) models, at the parameter values $r = 0.0$ (left panel), $r = 0.5$ (middle panel) and $r = 1.0$ (right panel) from $t = 0$ until $t = 5.0$. The results of the discrete simulations are given by the histograms, the output of the continuous model are given by dashed (initial distribution) and solid lines (final distribution). Observe the fair agreement between the discrete and the continuous models.

simulations. The evolution of the two parameters (respectively denoted to μ and σ) of the lognormal distribution are given in Figure 5 at values of the parameter r. The criticality of $r = 0.5$ is obvious in this setting, too: while the initially lognormal distribution is almost invariant under the evolution at $r = 1/2$, the evolution of the parameters μ and σ take an opposite direction in the parameter space for $r = 0.0$ and $r = 1.0$, respectively. The 95% confidence levels of the fit confirm the visual intuition: the evolved distributions are close to lognormal: in practical applications an approximation with a lognormal distribution produces an acceptable error.

3.3 Outliers: anomalies in smaller samples

The continuum model describes the $N \to \infty$ limit of the system. In the computations shown in Subsections 3.1 and 3.2 we either showed results based on the continuum model or, in the direct, discrete simulations we treated large ($N = 5000$) populations. However, if we look at the discrete simulations on smaller samples we may observe unexpected phenomena not recorded in the previous computations. In Fig. 6 we show the mass distribution of a system at $r = 0.6$ with $N = 2000$ particles. The bulk of the histograms can be well approximated with a log-normal distribution. However, there are 12 particles with somewhat larger volume than predicted by the lognormal distribution and one approximately 150 times the median volume (5.3 times the radius). Thus inside the focusing regime we may observe a situation where we have a well-defined narrow distribution which describes the bulk of the particles but a few might escape from this process and may be left behind, at larger mass. This effect is persistent and it was observed also for the parameter value of $r \simeq 0.7$.

In order to estimate the robustness of this scenario we use a simple approximation by assuming that all but one particles have volume X and one single, exceptional particle, called 'outlier' has a volume aX with $a \gg 1$. As it is demonstrated in Appendix

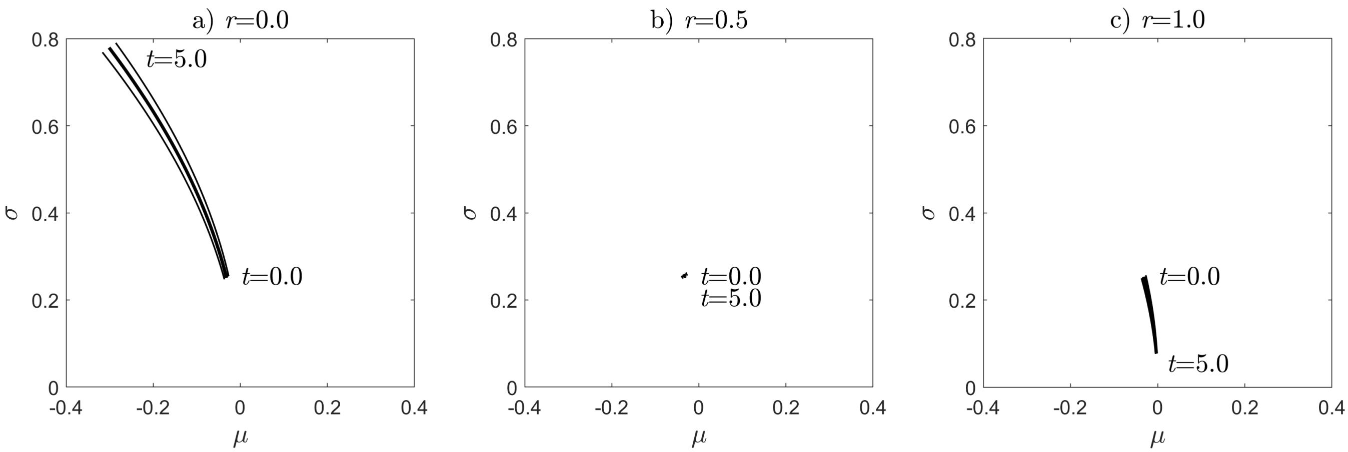

Figure 5. Parameters, μ and σ of a lognormal distributions fitted to the computed mass distribution in the compound model, at the parameter values $r = 0.0$ (left panel), $r = 0.5$ (middle panel) and $r = 1.0$ (right panel) from $t = 0$ until $t = 5.0$. Thick solid lines correspond to the best fit, thin lines indicate the 95% confidence level of the fit. Observe the narrow zone spanned by the confidence intervals.

E, the outlier can coexist with the population of the small particles. In the $N \to \infty$ limit the condition of such a coexistence reads

$$\frac{2a^r}{1+a} \leq 1. \tag{12}$$

Numerical solution of (12) for equality yields the *critical curve* $a_c(r)$ on the $[r, a]$ parameter plane, separating systems where outliers may coexist with the population from systems where they may not. While we computed the $a_c(r)$ critical curve for the case of infinitely large populations (the $N \to \infty$ limit), we stress the fact that the illustrated phenomenon is inherently discrete and does not arise in the continuum model. We may explain this curious phenomenon in the following manner. Assume that we start from a narrow distribution. Then random fluctuations in the discrete system may create particles with large relative mass (i.e., a large parameter value a). If these fluctuations are sufficiently large to create particles *above* the critical curve $a_c(r)$ then these outliers will be sustained, otherwise their mass will again approach the average mass of the majority. The critical curve in Figure 7. shows that in the vicinity of the critical value $r = 0.5$ almost any such fluctuation will be sustained and outliers are likely to survive. However, as the parameter r is increasing, it gets increasingly less likely to see sustained outliers. Another observation is that as the likelihood for the existence of outliers decreases, their expected relative size is increasing which matches the common-sense observation that the larger the outlier, the less frequently it may be observed. We also note that the relationship between the collection of small particles and the large particle is essentially asymmetrical. While the evolution of the latter is strongly influenced by both the factor a and the control parameter r, the evolution of the density function for the small particles is solely controlled by the latter. In other words, adding one (or a few) very large particles to a collection of many small particles will not alter the fate of the latter, as long as the collisions between a pair of particles are based on a uniform choice.

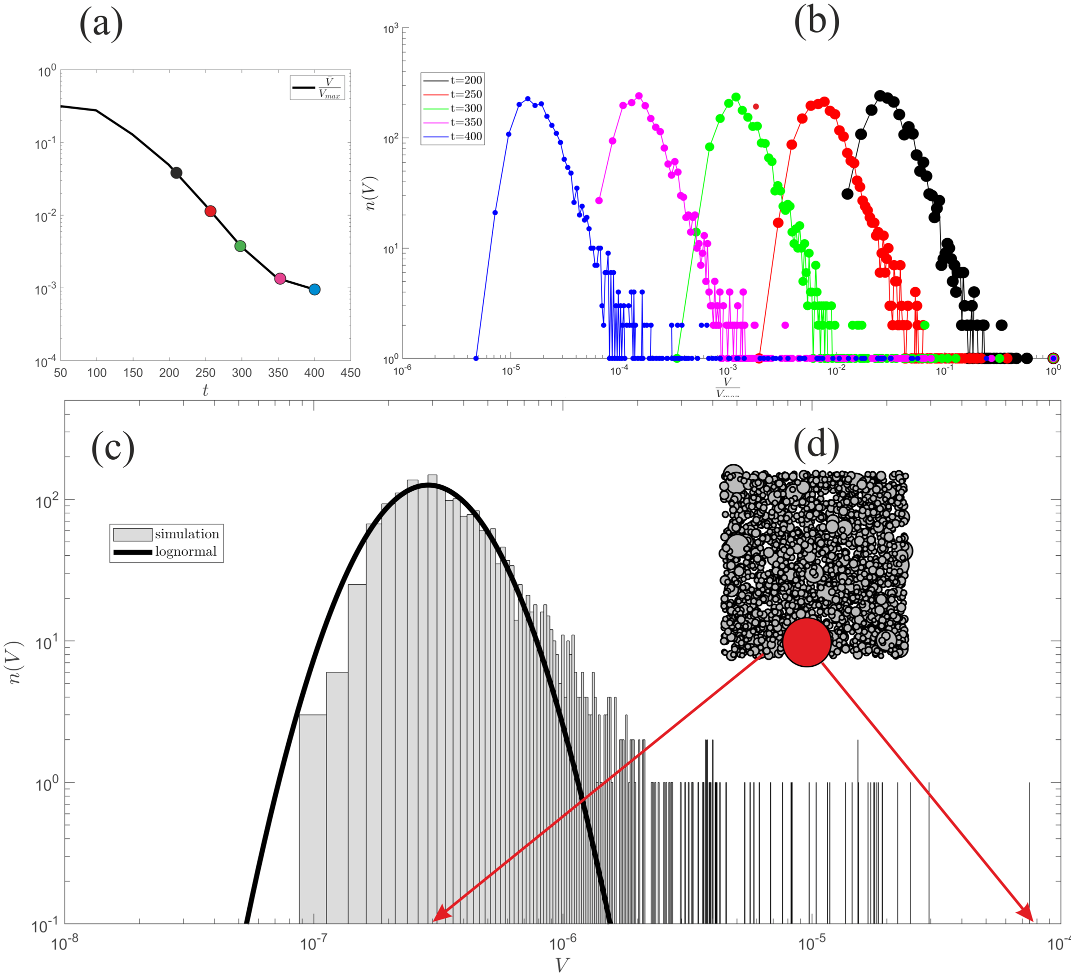

Figure 6. Simulation of a finite sample with $N = 2000$ particles. Inset (a) shows the evolution of the mean volume normalized by the maximal volume. Inset (b) depicts the evolution of the distribution, the corresponding points in (a) are denoted by the same color.The green curve ($t = 300$) is the one shown in detail in panel (c), it depicts the particle volume histogram after 300 collisions per particle. The grey boxes show the logarithmically binned histogram, the black line is a log-normal fit to the data. Observe the existence of outliers on the right. Inset (d) is a visual illustration of the entire population: all particles are placed randomly into a 2D container. Smaller particles were placed first and the white content (gray scale) is proportional to the linear size of the particle. One small particle close to the mean and one large particle (outlier) are marked with red and their position is indicated in the distribution.

4 Conclusions

In this paper we presented the first statistical model for the collective mass evolution of pebble populations under collisional abrasion. While our model is certainly not unique, it is compatible with

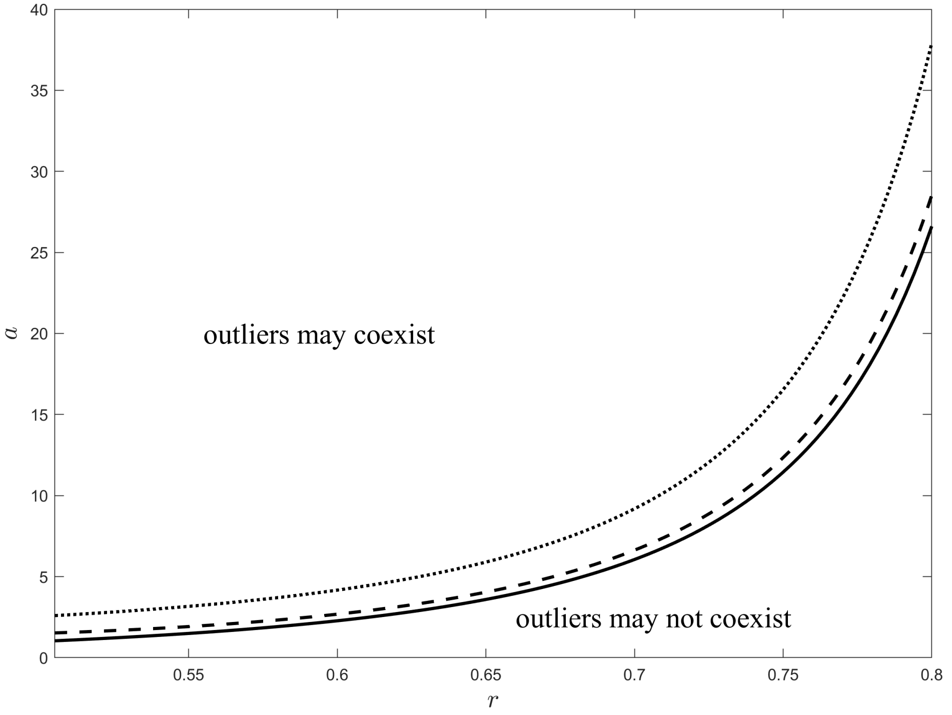

Figure 7. Critical curve $a_c(r)$ on the $[r, a]$ parameter plane. Systems with parameters (r, a) associated with points above the curve admits the coexistence of outliers while the systems associated with points below the critical curve do not admit the coexistence of outliers. Solid line belongs to the $N \to \infty$ limit, dotted line represents $N = 20$ and the dashed line $N = 100$ particles, respectively.

(a) existing geological observations,

(b) existing geometrical theory of individual and binary abrasion of pebbles,

(c) existing theory for individual mass evolution of pebbles (Sternberg's Law) and

(d) exiting statistical theory of coagulation and fragmentation.

In the spirit of standard statistical theory for collective evolution, our model is based on two components: (i) the binary collision kernel and, based on the latter, (ii) the governing equation for the evolution of probability density functions for mass distribution. Regarding (i) we used the model from (Domokos and Gibbons, 2018) which incorporates the existing theory for individual and binary abrasion, regarding (ii) we used the Fokker-Planck equation which is broadly used in the theory of coagulation in fragmentation.

Our collision kernel includes the single scalar parameter r which can be associated with the energy level of the collective collisional evolution process. We found that $r = 0.5$ is *critical*, separating two regimes with fundamentally different behaviour: for $r > 0.5$ (low energy regime) we found *focusing* behaviour with *decreasing relative variance* $R(t)$ and for $r < 0.5$ (high energy regime) we found *dispersing* behaviour with *increasing relative variance* $R(t)$. In geological terms, this result suggests that in low energy environments collisional abrasion acts on mass distributions in unison with size-selective transport while in high energy environments the opposite happens and the two processes are counter-acting. In accordance with prevailing geological observations and Sternberg's Law,, our models predicts exponential decay of particle mass in both energy regimes.

We investigated our model on two levels: (i) as a continuum model by regarding the evolution of the Fokker-Planck equation and (ii) as a discrete model by running discrete event-based simulations. In case of the continuum model we derived our results analytically and also from numerical simulation of the Fokker-Planck equation while in the discrete model we relied on numerical computations. In regard of the existence of the critical parameter $r = 0.5$ and the existence of the focusing and dispersing regimes, the two approaches yielded quantitatively matching results.

Large boulders among many small pebbles are often visible in mountain ranges of rivers. While this phenomenon is commonly attributed to transport, our model suggests that under some conditions, here again transport and abrasion may act in unison: we identified a curios phenomenon *not* present in the continuum model but present in the discrete model (even in the $N \to \infty$ limit). If the parameter r was in the focusing $r > 0.5$ range but not very far from the critical value $r = 0.5$, the bulk of the distribution was narrowing (in accordance with our analytical predictions), however, we could also observe a few particles with substantially larger mass (outliers), escaping the bulk of the distribution. We characterized the mass ratio of outliers versus the mean of the bulk distribution by the parameter a and we derived a *critical curve* $a_c(r)$ separating systems where outliers may be observed from those where this may not happen. Our result predicts that larger outliers are less likely to be observable.

While our paper only dealt with on size distributions, however, there exist also related observations on shape: sharp peaks in distributions of axis ratios (also referred to as *equilibrium shapes*) are mentioned in Bluck (1967); Dobkins and Folk (1970); Landon (1930); Orford (1975); Williams and Caldwell (1988); Ashcroft (1990); Lorang and Komar (1990); Yazawa (1990); Wald (1990). In Domokos and Gibbons (2012) a plausible argument was presented that equilibrium shapes may emerge on shingle beaches as the result of interaction of abrasion and transport. We hope that the extension of the statistical theory presented in this paper may be capable to verify these observations.

Appendix A: Testing the model for heterogeneous pebble populations

In the context of the binary evolution model (1)-(2) we introduced the binary abrasion parameters c_{12} and c_{21} and for simplicity (since we only aimed to treat homogeneous populations) we used the same notation in the collision kernel (3)-(4). Here we refine this concept in the statistical setting for heterogeneous populations where we regard the collective evolution of N particles with $M \leq N$ different materials m_i, $(i = 1, 2, \ldots M)$. (The binary case corresponds to $N = 2$, if the two pebbles are made from different material then we have $M = 2$ and for pebbles with identical materials we have $M = 1$. In the latter case in (1)-(2) we have $c_{12} = c_{21} = c$.)

In the statistical setting the binary abrasion parameters can be organized into an $M \times M$ matrix $\mathcal{M}$ with entries c_{ij}, $(i, j = 1, 2, \ldots M)$. The binary parameter c_{ij} is defined as the constant coefficient in the collision kernel (3)-(4) associated with the abrasion rate of a particles with material m_i, bombarded by particles with material m_j. Needless to say, the matrix $\mathcal{M}$ is not symmetrical, in general we have $c_{ij} \neq c_{ji}$. In particular, if material m_i is much harder than material m_j then we expect $c_{ij} \ll c_{ji}$.

Based on the above considerations, the statistical model is controlled by the $M \times M = M^2$ binary abrasion parameters and the single environmental parameter r. Testing this model can be done along the strategies outlined in subsection 1.4 for homogeneous populations, however, more detail has to be observed.

(a) One may test the model at the *input level*, by fitting the kernel (3)-(4) to laboratory tests for pair-wise selected materials m_i, m_j. In such a test the abrasion rate of particles of material m_i under abrasion from particles of material m_j is plotted as a function of particle size of the abraded particle (with material m_i). Such experiments can be used to determine the binary abrasion parameters c_{ij} for a given heterogeneous population. If the laboratory test is imitating the environment of the natural process, the environmental parameter r may be also obtained in this manner. We will show such an example below.

(b) One may test the model at the *output level* by measuring the time evolution of full mass distributions and fitting the M^2 material parameters c_{ij} and the environmental parameter r to this dataset.

Next we show an example for testing the model at the input level by using the data obtained in Attal and Lavé (2009). Here the authors report on flume experiments where they measured the abrasion rate E_d of individual limestone gravels with diameter between $D = 9$ and $D = 39$ mm mixed in approximately 400g of 10-18 mm and 18-28 mm granitic gravel. In our terminology, we have $M = 2$ (two materials) and we will use m_1 for the limestone and m_2 for the granite. The joint evolution of such a heterogeneous population is described by $M^2 = 4$ binary material constants: c_{11}, c_{12}, c_{21} and c_{22}. The authors were primarily interested in the abrasion rates for limestone and they produced the $E_d(D)$ plots for these particles. In this experiment we may assume that the abrasion of the limestone pebbles was exclusively due to collisions with the granitic gravel (i.e. we disregard limestone-limestone collisions). Thus the only relevant collisions are between limestone and granite, and for the mass loss $X(t)$ of the limestone we will use equation (3) with X and Y denoting the volumes of the colliding limestone and granitic particles respectively, and c_{12} denoting the binary abrasion parameter associated with limestone being abraded by granite. (Not reported, by we may assume $c_{21} \ll c_{12}$). If we replace the volume of the granitic particles by their average the abrasion rate as function of its diameter can be calculated numerically. Note that the abrasion rate E_d in our notation reads

$$E_d = -\frac{X_t}{X}. \tag{A1}$$

We fitted equation (3) to the dataset provided in Attal and Lavé (2009). We minimized the mean square error (with respect to the results in Attal and Lavé (2009)) for the parameters r and c_{12} and obtained $r = 0.19, c_{12} = 0.28$. Our fitted curves are illustrated in Figure A1 showing fair agreement between the data and the fitted model. The value of the environmental parameter is in the range where we expect dispersing behaviour, as we discussed in Appendix D, which is in accordance with the target of the original experiment which simulated abrasion in fluvial environments. We note that the same parameter-pair $r = 0.19, c_{12} = 0.28$ is valid for both limestone experiments (i.e. these parameters do not depend on the size of the particle). Our fit appears to be consistent in this respect.

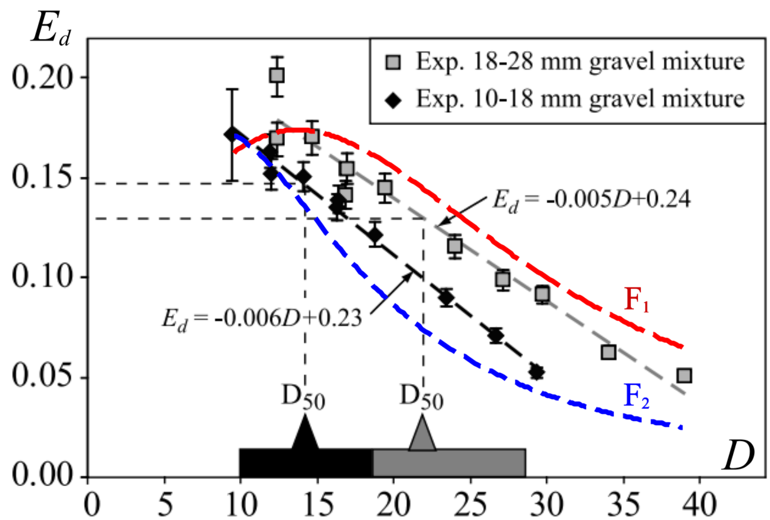

Figure A1. (a) Abrasion rate E_d predicted by the compound kernel (3) fitted to experimental data in Attal and Lavé (2009). Figure 9a by Attal and Lavé (2009) superposed with our model fits F_1 and F_2. Mass estimated from diameter. Least squares optimization yields $r = 0.19$ and $c_{12} = 0.28$.

Appendix B: Some properties of the kernels in Subsection 2.3

B1 Summation kernel

Differential equations governing the time evolution of the first and second moments can be readily obtained, hence the mean $E^+(t)$ and variance $W^+(t)$ follows the following initial value problems (IVPs):

$$E_t^+(t) = -2E^+(t) \quad \text{with} \quad E^+(0) = E_0, \tag{B1}$$

$$W_t^+(t) = -2W^+(t) \quad \text{with} \quad W^+(0) = W_0. \tag{B2}$$

It follows, that both the expectation and the variance exhibit exponential decay, namely $E^+(t) = E_0 e^{-2t}$ and $W^+(t) = W_0 e^{-2t}$. It is straightforward to show, that the relative variance $R^+(t)$ increases exponentially

$$R^+(t) := \frac{W^+(t)}{E^+(t)^2} = \frac{W_0}{E_0^2} e^{2t} = R_0 e^{2t}. \tag{B3}$$

B2 Product kernel

In case of the product kernel the IVPs describing the evolution of the mean $E^*(t)$ and variance $W^*(t)$ respectively read

$$E_t^*(t) = -(E^*(t))^2 \qquad \text{with} \qquad E^*(0) = E_0, \tag{B4}$$

$$W_t^*(t) = -2W^*(t)E^*(t) \quad \text{with} \quad W^*(0) = W_0. \tag{B5}$$

Here the decay of the mean and the variance are polynomial as we find

$$E^*(t) = \frac{1}{t+\dfrac{1}{E_0}}, \quad \text{and} \quad W^*(t) = \frac{W_0}{E_0}^2 \frac{1}{\left(t+\dfrac{1}{E_0}\right)^2}. \tag{B6}$$

which result in a steady relative variance $R^*(t)$, determined by the initial distribution f_0. In specific

$$R^*(t) := \frac{W^*(t)}{E^*(t)^2} = \frac{W_0}{E_0^2} = R_0. \tag{B7}$$

Appendix C: Approximate investigation of the compound kernel

C1 Truncated compound kernel

The truncated compound kernel is obtained from the compound kernel as the truncated Taylor polynomial computed at $y = x$ with an $(O(y-x)^2$:

$$\psi^{c,T}(x,y) := \frac{x}{2} + \left(\frac{1}{4} - \frac{r}{2}\right)(y-x) + O((y-x)^2). \tag{C1}$$

Using the master equation, the following Cauchy problems are found that define the evolution of the mean and the variance:

$$E_t^{c,T}(t) = -\frac{1}{2}E^{c,T}(t) \qquad \text{with} \qquad E^{c,T}(0) = E_0, \tag{C2}$$

$$W_t^{c,T}(t) = -\left(\frac{1}{2}+r\right)W^{c,T}(t) \quad \text{with} \quad W^{c,T}(0) = W_0. \tag{C3}$$

Solution of these ODEs yields the evolution of the relative variance as

$$R^{c,T}(t) := \frac{W^{c,T}(t)}{E^{c,T}(t)^2} = \frac{W_0}{E_0^2} e^{\left(\frac{1}{2}-r\right)t}. \tag{C4}$$

C2 A population of identical particles preserved

Here we show, that a population of identical particles, characterized by a Dirac delta function as P.D.F. is preserved in the model with the compound kernel regardless of the value of parameter r. Without loss of generality, we investigate the evolution from the $f_0 = \delta(1)$ initial condition, where $\delta(x)$ denotes the Dirac-delta function at x. Obviously, $E_0 = 1$ and $W_0 = 0$. We show, that now $f(t,x) = \delta(c(t))$ holds for any $t > 0$. Let us assume, that at some $t^* \geq 0$ the distribution is $f(t^*,x) = \delta(c(t^*))$ with mean $E^c(t^*) = c(t^*)$ and variance $W^c(t^*) = 0$, respectively. Observe that

$$\int_0^\infty f(t^*,y)\psi^c(x,y)dy = \psi^c(x,c(t^*)). \tag{C5}$$

The time derivative of the mean can be computed via

$$E_t^c(t^*) = \int_0^\infty f_t(t^*,x)x\,dx = -\int_0^\infty f(t^*,x)\psi^c(x,c(t^*))dx = -\frac{1}{2}c(t^*), \tag{C6}$$

where we used (7), applied integration by parts and employed (C5). Similarly, the evolution of the variance is found to follow:

$$W_t^c(t^*) = \int_0^\infty f_t(t^*,x)x^2dx - 2E_t^c(t^*)E^c(t^*) = -2\int_0^\infty f(t^*,x)\psi^c(x,c(t^*))xdx + c(t^*)^2 = -c(t^*)^2 + c(t^*)^2 = 0. \tag{C7}$$

This shows that the variance of the distribution is constant, and as it started at $W_0 = 0$, i.e. it vanishes whole along the evolution. In other words, the we have a Dirac-delta (degenerate) distribution at any $t \geq 0$. Employing (C6) we find, that the location $c(t)$ follows the initial value problem $c_t(t) = -\frac{1}{2}c(t)$ with $c(0) = 1$, hence $c(t) = \exp(-\frac{t}{2})$.

C3 Dispersing and focusing behaviour identified in the population of almost identical particles

As the model lacks diffusion, the behaviour of a degenerate distribution with all the mass concentrated at a single value is worthy to study. In Appendix C2 we show that a population of identical particles remain identical in our model. In other words, time-invariance of the Dirac-delta distribution holds in our model, regardless of the value of the parameter r. Nevertheless, the value of r affects the *stability* of that Dirac-delta: next we show that the evolution for a population of *almost* identical particles (i.e. a perturbed version of the Dirac delta distribution) is either focusing or dispersing, depending on the value of r. To see this, we define a perturbed distribution. Let $\varepsilon > 0$ be a fixed parameter and define

$$\hat{f}_0(x) := \begin{cases} (1-\varepsilon)\delta(1) + \frac{1}{2} & \text{if } 1-\varepsilon \leq x \leq 1+\varepsilon \\ 0 & \text{otherwise .} \end{cases} \tag{C8}$$

It is straightforward to show that $\int_0^\infty \hat{f}_0(y)\psi^c(x,y)dy = \psi^c(x,1)$, $E_0^c = 1$ and $M_2^c(t) := \int_0^\infty f(t,x)x^2dx$ with $M_2^c(0) = 1 + \frac{1}{3}\varepsilon^3$. We aim to investigate the sign of R_t^c at $t = 0$. Since $R^c(t) = M_2^c(t)E^c(t)^{-2} - 1$, we need to study the sign of $M_{2,t}^c(0)E^c(0) - 2E_t^c(0)M_2^c(0)$. Integration by parts yields

$$E^c(0)M_{2,t}^c(0) - 2M_2^c(0)E_t^c(0) = -2\int_0^\infty \hat{f}_0(x)\psi^c(x,1)xdx + 2(1+\frac{1}{3}\varepsilon^3)\int_0^\infty \hat{f}_0(x)\psi^c(x,1)dx = \frac{1}{3}\varepsilon^3\left(\frac{1}{2} - r\right) + O(\varepsilon^3), \tag{C9}$$

where algebraic manipulations leads the last equality. In accordance with the results on the truncated model, we found, that $r = 1/2$ is critical, at $r < 1/2$ the relative variance R_t^c is positive, it increases for any $\varepsilon > 0$, i.e. the population of identical particles is *unstable*, small perturbations disperse the mass distribution. At $r > 1/2$ the relative variance $R_t^c < 0$, which shows, that the population of identical particles is *stable*, the model is focusing.

Appendix D: Estimating physically possible values of r

In the paper we assumed that the particle collision probability depends on the volume of the particles as

$$P(X) \propto X^r. \tag{D1}$$

Here we investigate two extreme scenarios, associated with the collision probabilities $P_{\text{smooth}}(X)$ and $P_{\text{turbulent}}(X)$ where we expect r to assume its extreme values.

The first is the smooth gradient flow. In such a case the driving fluid has a strong, but on a particle-size scale constant velocity gradient in one of the spatial directions. Such situations may arise, e.g., in shallow water layers. Here the relative velocity of the particles grows with the distance. If we are at distance u from the center of the particle in the direction of the flow velocity gradient, the collision probability $P_{\mathrm{smooth}}(X)$ can be estimated by the product of the velocity difference and the linear cross-section of the particles. (Note that $R \equiv X^{1/3}$ is the linear size of the particle):

$$P_{\mathrm{smooth}}(X) \sim \frac{1}{R}\int_0^R u\sqrt{R^2-u^2}du = \frac{1}{3}R^2 = \frac{1}{3}X^{2/3}. \tag{D2}$$

Based on (D1), this gives us an estimate for high $r = 2/3$.

The other extreme case is a fully chaotic motion where equipartition takes place Uberoi (1957). Thus the kinetic energy of the particles ($\frac{1}{2}\rho X v^2$) is independent of their volume. Thus the speed of the particles must be proportional to $X^{-1/2}$. If we disregard correlations the particles have a cross-section proportional to their projected area which is proportional to $X^{2/3}$. Combining the two gives us

$$P_{\mathrm{turbulent}}(X) \sim X^{-1/2}X^{2/3} = X^{1/6} \tag{D3}$$

and based on (D1) we obtain $r = 1/6$. Thus it is possible to have physical scenarios apparent in nature where the value of r falls to either side of the critical value of $r_c = 0.5$ with large enough margin.

Appendix E: Investigation of outliers in finite samples

Let us have a sample with N particles with $(N-1)$ having identical volume X. The last particle is an outlier with volume aX, where $a \ll 1$. In a single binary collision, a hit between particles with volume X is called an A-type event, while a collision with the outlier being involved is a B-type event. Based on discrete probabilistic considerations, the probability of an A-type event equals $(N-2)/N$ and a B-type event is $2/N$, respectively. In the A-type event the average size $\bar{X}$ of the particles with volume X after the collision that lasts for Δt reads

$$\bar{X} = \frac{2(X - X/2\Delta t) + (N-3)X}{N-1} = X - \frac{X}{N-1}\Delta t. \tag{E1}$$

Computing $aX/\bar{X}$ and truncating the Taylor series expansion in Δt after linear terms around the value $\Delta t = 0$ yields the time derivative of the parameter a associated with an A-type event:

$$a_t^A = \frac{a}{N-1}. \tag{E2}$$

In case of the B-type event both the outlier and one of the small particles follow the compound kernel via:

$$(aX)_t = -\frac{a^{1+r}X}{1+a}, \tag{E3}$$

$$X_t = -\frac{a^{1-r}X}{1+a}. \tag{E4}$$

The second equation is employed to compute the average volume of the small particles (i.e., $\bar{X}$ associated with this event). Now we need to truncate the Taylor series of $\frac{aX-(aX)_t\Delta t}{X-\bar{X}}$ at $\Delta t = 0$. After algebraic manipulations we find

$$a_t^B = -\frac{a^{1+r}}{1+a} + \frac{a^{2-r}}{(1+a)(N-1)}. \tag{E5}$$

Considering the probabilities of events A and B we arrive to

$$a_t = a\frac{N-2}{N-1} - 2\left(\frac{a^{1+r}}{1+a} + \frac{a^{2-r}}{(1+a)(N-1)}\right). \tag{E6}$$

Note that an increase in the value of a, i.e., $a_t > 0$ implies that the outlier is getting further from the population. In the case of the $N \to \infty$ limit we find

$$a_t = a\left(1 - \frac{2a^r}{1+a}\right). \tag{E7}$$

Here the sign of the expression in the brackets determines the sign of a_t, which coincides with e.q. (12) in the text. One can also show, that if there exist $a^c > 1$ such that $a_t = 0$ at a_c, then $a_t > 0$ for any $a > a^c$. Hence, we need the $a_c > 1$ that makes the expression in the bracket vanish. Existence of such a critical value can be shown for the case with finitely many particles, too.

Author contributions. G.D. proposed the problem and supervised the research; A.Á.S. carried out the analytical and numerical study of the continuous model, T.J. developed the discrete numerical model; G.D., A.Á.S. and J.T. wrote the paper.

Competing interests. The authors declare that they have no competing interests.

Acknowledgements. The authors are indebted to the referees D. Furbish, S. Carretier and D. Bertoni. Responding to their commenst helped to improve the manuscript substantially. The authors sincerely thank J. Lavé and M. Attal for sharing the original dataset of their abrasion experiments. The research reported in this paper was supported by the BME Water Sciences & Disaster Prevention TKP2020 IE grant of NKFIH Hungary (BME IE-VIZ TKP2020) and the NKFIH grant K134199.

References

Ashcroft, W.: Beach pebbles explained, Nature, 346, 227, 1990.

Attal, M. and Lavé, J.: Changes of bedload characteristics along the Marsyandi River (central Nepal): Implications for understanding hillslope sediment supply, sediment load evolution along fluvial networks, and denudation in active orogenic belts, in: Tectonics, Climate, and Landscape Evolution, Geological Society of America, 2006.

Attal, M. and Lavé, J.: Pebble abrasion during fluvial transport: Experimental results and implications for the evolution of the sediment load along rivers, Journal of Geophysical Research: Earth Surface, 114, 2009.

Bertoni, D., Sarti, G., Grottoli, E., Ciavola, P., Pozzebon, A., Domokos, G., and Novák-Szabó, T.: Impressive abrasion rates of marked pebbles on a coarse-clastic beach within a 13-month timespan, Marine Geology, 381, 175 – 180, 2016.

Bird, E.: Lateral Grading of Beach Sediments: A Commentary., Journal of Coastal Research, 12, 774–785, 1996.

Bloore, F. J.: The Shape of Pebbles, Math. Geol., 9, 113–122, 1977.

Bluck, B. J.: Sedimentation of beach gravels; examples from South Wales, Journal of Sedimentary Research, 37, 128–156, 1967.

Brewer, P. A. and Lewin, J.: In-Transport Modification of Alluvial Sediment: Field Evidence and Laboratory Experiments, pp. 23–35, John Wiley & Sons, Ltd, 1993.

Carr, A. P.: Size grading along a pebble beach; chesil beach, England, Journal of Sedimentary Research, 39, 297–311, 1969.

Cheng, Z. and Redner, S.: Scaling Theory of Fragmentation, Phys. Rev. Lett., 60, 2450–2453, 1988.

da Costa, F. P.: Mathematical Aspects of Coagulation-Fragmentation Equations, in: Mathematics of Energy and Climate Change, edited by Bourguignon, J.-P., Jeltsch, R., Pinto, A. A., and Viana, M., pp. 83–162, Springer International Publishing, Cham, 2015.

Dingle, E. H., Attal, M., and Sinclair, H. D.: Abrasion-set limits on Himalayan gravel flux, Nature, 544, 471—474, https://doi.org/10.1038/nature22039, 2017.

Dobkins, J. E. and Folk, R. L.: Shape development on Tahiti-Nui, Journal of Sedimentary Research, 40, 1167–1203, 1970.

Domokos, G. and Gibbons, G. W.: The evolution of pebble size and shape in space and time, Proc. Roy. Soc. A., 468, 3059–3079, 2012.

Domokos, G. and Gibbons, G. W.: The Geometry of Abrasion, in: New Trends in Intuitive Geometry, edited by Ambrus, G., Bárány, I., Böröczky, K. J., Fejes Tóth, G., and Pach, J., pp. 125–153, Springer Berlin Heidelberg, Berlin, Heidelberg, 2018.

Driscoll, T. A., Hale, N., and Trefethen, L. N.: Chebfun Guide, Pafnuty Publications, Oxford, 2014.

Ernst, M. H. and Pagonabarraga, I.: The Nonlinear Fragmentation Equation, J. Physics A. Math. Theo., 40, F331–F337, 2007.

Fedele, J. J. and Paola, C.: Similarity solutions for fluvial sediment fining by selective deposition, Journal of Geophysical Research: Earth Surface, 112, 2007.

Ferguson, R., Hoey, T., Wathen, S., and Werritty, A.: Field evidence for rapid downstream fining of river gravels through selective transport, Geology, 24, 179–182, 1996.

Firey, W. J.: Shapes of worn stones, Mathematika, 21, 1–11, 1974.

Gleason, R., Blackley, M. W. L., and Carr, A. P.: Beach stability and particle size distribution, Start Bay, Journal of the Geological Society, 131, 83–101, 1975.

Hansom, J. D. and Moore, M. P.: Size Grading along a Shingle Beach in Wicklow, Ireland, Journal of Earth Sciences, 4, 7–15, 1981.

Huber, M. L., Lupker, M., Gallen, S. F., Christl, M., and Gajurel, A. P.: Timing of exotic, far-traveled boulder emplacement and paleo-outburst flooding in the central Himalayas, Earth Surface Dynamics, 8, 769–787, https://doi.org/10.5194/esurf-8-769-2020, 2020.

Kuenen, P. H.: Experimental Abraison: 6. Surf Action, Sedimentology, 3, 29–43, 1964.

Kuenen, P. H. and Migliorini, C. I.: Turbidity Currents as a Cause of Graded Bedding, The Journal of Geology, 58, 91–127, 1950.

Landon, R. E.: An Analysis of Beach Pebble Abrasion and Transportation, The Journal of Geology, 38, 1930.

Lewis, W. V.: The Effect of Wave Incidence on the Configuration of a Shingle Beach, The Geographical Journal, 78, 129–143, 1931.

Lorang, M. and Komar, P.: Pebble shape, Nature, 347, 433–434, 1990.

Lubachevsky, B. D.: How to simulate billiards and similar systems, Journal of Computational Physics, 94, 255 – 283, 1991.

Meyer, C. J. and Deglon, D. A.: Particle collision modeling – A review, Minerals Engineering, 24, 719 – 730, 2011.

Miller, K. L., Szabó, T., Jerolmack, D. J., and Domokos, G.: Quantifying the significance of abrasion and selective transport for downstream fluvial grain size evolution, Journal of Geophysical Research: Earth Surface, 119, 2412–2429, 2014.

Neate, D. J. M.: Underwater pebble grading of Chesil Bank, Proceedings of the Geologists' Association, 78, 419 – 426, 1967.

Novák-Szabó, T., Sipos, A. Á., Shaw, S., Bertoni, D., Pozzebon, A., Grottoli, E., Sarti, G., Ciavola, P., Domokos, G., and Jerolmack, D. J.: Universal characteristics of particle shape evolution by bed-load chipping, Science Advances, 4, https://doi.org/10.1126/sciadv.aao4946, https://advances.sciencemag.org/content/4/3/eaao4946, 2018.

Orford, J. D.: Discrimination of particle zonation on a pebble beach, Sedimentology, 22, 441–463, 1975.

Paola, C., Parker, G., Seal, R., Sinha, S. K., Southard, J. B., and Wilcock, P. R.: Downstream fining by selective deposition in a laboratory flume, Science, 258, 1757–1760, 1992.

Sternberg, H.: Untersuchungen uber Langen-und Querprofilgeschiebefuhrender Flusse, Z. Bauwes., 25, 486–.506, 1875.

Szabó, T., Fityus, S., and Domokos, G.: Abrasion model of downstream changes in grain shape and size along the Williams River, Australia, Journal of Geophysical Research: Earth Surface, 118, 2059–2071, https://doi.org/10.1002/jgrf.20142, 2013.

Szabó, T., Domokos, G., Grotzinger, J. P., and Jerolmack, D. J.: Reconstructing the transport history of pebbles on Mars, Nature Communications, 6, 8366, 2015.

Uberoi, M. S.: Equipartition of energy and local isotropy in turbulent flows, Journal of Applied Physics, 28, 1165–1170, 1957.

Wald, Q. R.: The form of pebbles, Nature, 345, 211, 1990.

Whittaker, A. C., Duller, R. A., Springett, J., Smithells, R. A., Whitchurch, A. L., and Allen, P. A.: Decoding downstream trends in stratigraphic grain size as a function of tectonic subsidence and sediment supply, GSA Bulletin, 123, 1363–1382, 2011.

Williams, A. T. and Caldwell, N. E.: Particle size and shape in pebble-beach sedimentation, Marine Geology, 82, 199 – 215, 1988.

Yazawa, T.: More pebbles, Nature, 348, 398, 1990.